Electrochemical and Fluorescence Sensing Performance of Four New Coordination Polymers Tuned by Different Metal Ions and Dicarboxylic Acids

Xiuli Wang*, Yue Wang, Na Xu, Jianxin Ma, Guocheng Liu

†College of Chemistry and Materials Engineering, Bohai University, Professional Technology Innovation Centre of Liaoning Province for Conversion Materials of Solar Cell, Jinzhou 121013, P. R. China.

Synthesis of the Ligand 4-dptb. 3,4-Thiophenedicarboxylic acid (4.4 g) and 4-picolinylamine (4.7 g) were mixed in 50 mL of pyridine. Then the mixture was stirred for 30 min and 9 mL of triphenyl phosphite was added. After refluxing for 10 h and sitting overnight, a white powder was obtained by repeated cleaning and filtration with pyridine at room temperature.

X-ray crystallography. Data collection was performed on Bruker Smart APEX II diffractometer with Kα (λ = 0.71073 Å) by θ and ω scan mode at room temperature. The structure was solved by using direct methods and refined by full-matrix least-squares methods on F^2 using the olex-2 software[1]. Anisotropic thermal parameters were utilized in all non-hydrogen atoms. CCDC No. 2155858, 2155859, 2180652, and 2155857. Selected bond lengths and angles were shown in Table S1-S4 for CPs **1**–**4**.

Table S1 Bond lengths [Å] and angles [°] for CP 1.

Zn(1)-O(2)	1.9399(18)	Zn(2)-O(1)	1.9388(18)
Zn(1)-O(3)	1.9208(18)	Zn(2)-O(4)	1.9242(18)
Zn(1)-N(4)#1	2.023(2)	Zn(2)-N(1)#2	2.024(2)
Zn(1)-N(6)	2.016(2)	Zn(2)-N(3)	2.015(2)
O(2)-Zn(1)-N(4)#1	99.55(8)	C(1)-O(1)-Zn(2)	120.25(16)
O(2)-Zn(1)-N(6)	104.50(8)	C(23)-O(2)-Zn(1)	121.54(17)
O(3)-Zn(1)-O(2)	132.29(8)	C(16)-O(3)-Zn(1)	122.24(17)
O(3)-Zn(1)-N(4)#1	100.33(8)	C(24)-O(4)-Zn(2)	125.97(18)
O(3)-Zn(1)-N(6)	103.37(9)	C(4)-N(1)-Zn(2)#1	121.80(18)
N(6)-Zn(1)-N(4)#1	118.19(9)	C(22)-N(1)-Zn(2)#1	120.21(17)
O(1)-Zn(2)-N(1)#2	103.09(8)	C(28)-N(3)-Zn(2)	118.24(19)
O(1)-Zn(2)-N(3)	107.65(8)	C(39)-N(3)-Zn(2)	124.89(19)
O(4)-Zn(2)-O(1)	128.34(8)	C(10)-N(4)-Zn(1)#2	120.21(18)
O(4)-Zn(2)-N(1)#2	100.85(8)	C(26)-N(4)-Zn(1)#2	121.76(18)
O(4)-Zn(2)-N(3)	100.50(9)	C(37)-N(6)-Zn(1)	120.75(19)
N(3)-Zn(2)-N(1)#2	117.48(9)	C(50)-N(6)-Zn(1)	122.04(19)

Symmetry code: #1x+1,y,z; #2 x-1,y,z.

Table S2 Hydrogen-bonding parameters of CP 1.

D-H···A	D-H	H···A	D···A	D-H···A
O3-H3···N5	2.029(3)	0.86(4)	2.849(5)	142.3
O9-H9···N2	2.046	0.860	2.849	156.8

Table S3 Bond lengths [Å] and angles [°] for CP 2.

Cd(1)-O(1)#1	2.299(3)	Cd(1)-O(9)	2.233(3)
Cd(1)-O(1W)	2.246(3)	Cd(1)-N(2)	2.362(3)
Cd(1)-O(2W)	2.367(3)	Cd(1)-N(3)#1	2.388(3)
O(1)#1-Cd(1)-O(2W)	89.99(11)	O(1W)-Cd(1)-N(3)#1	93.99(12)
O(1)#1-Cd(1)-N(2)	164.63(11)	O(2W)-Cd(1)-N(3)#1	84.93(12)
O(1)#1-Cd(1)-N(3)#1	81.74(11)	O(9)-Cd(1)-O(1)#1	106.05(12)
O(1W)-Cd(1)-O(1)#1	90.37(10)	O(9)-Cd(1)-O(1W)	93.92(13)
O(1W)-Cd(1)-O(2W)	178.81(12)	O(9)-Cd(1)-O(2W)	87.08(14)
O(1W)-Cd(1)-N(2)	92.84(11)	O(9)-Cd(1)-N(2)	88.73(12)
O(9)-Cd(1)-N(3)#1	168.86(13)		
Symmetry code: #1 x+1,y,z-1; #2 x-1,y,z+1			

Table S4 Bond lengths [Å] and angles [°] for CP 4.

Co(1)−O(1)#1	2.112(5)	Co(1)−O(4)	2.083(5)
Co(1)−O(2)	2.082(5)	Co(1)−N(1)	2.193(6)
Co(1)−O(3)#2	2.107(5)	Co(1)−N(2)#3	2.205(6)
O(1)#1−Co(1)−N(1)	81.8(2)	O(4)−Co(1)−N(1)	90.4(2)
O(1)#1−Co(1)−N(2)#3	92.6(2)	O(4)−Co(1)−N(2)#3	98.7(2)
O(2)−Co(1)−O(1)#1	175.9(2)	N(1)−Co(1)−N(2)#3	169.4(2)
O(2)−Co(1)−O(3)#2	88.3(2)	C(2)−O(1)−Co(1)#2	125.4(5)
O(2)−Co(1)−O(4)	93.0(2)	C(2)−O(2)−Co(1)	136.0(5)
O(2)−Co(1)−N(1)	96.5(2)	C(1)−O(3)−Co(1)#1	126.5(5)
O(2)−Co(1)−N(2)#3	88.5(2)	C(1)−O(4)−Co(1)	132.2(5)
O(3)#2−Co(1)−O(1)#1	88.04(19)	C(15)−N(1)−Co(1)	119.4(5)
O(3)#2−Co(1)−N(1)	90.5(2)	C(15)−N(1)−C(16)	117.3(7)
O(3)#2−Co(1)−N(2)#3	80.2(2)	C(16)−N(1)−Co(1)	122.4(5)
O(4)−Co(1)−O(1)#1	90.7(2)	C(5)−N(2)−Co(1)#4	120.9(5)
O(4)−Co(1)−O(3)#2	178.3(2)		
Symmetry code: #1 -x+1/2,y+1/2,z; #2 -x+1/2,y-1/2,z; #3 x,-y+1/2,z+1/2; #4 x,-y+1/2,z-1/2			

Table S5 The Ksv values of CPs 1–2 for sensing $Cr_2O_7^{2-}$ and CrO_4^{2-} anions.

Complex	$Cr_2O_7^{2-}$ anions (M^{-1})	CrO_4^{2-} anions (M^{-1})
CP **1**	2.836×10^3	4.74×10^3
CP **2**	1.85×10^3	2.57×10^3

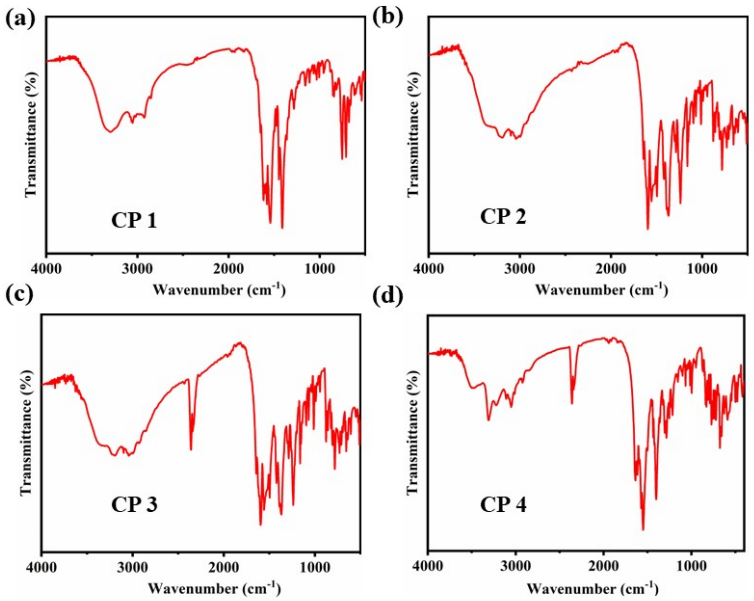

Figure S1. The IR spectra of CPs **1**–**4**.

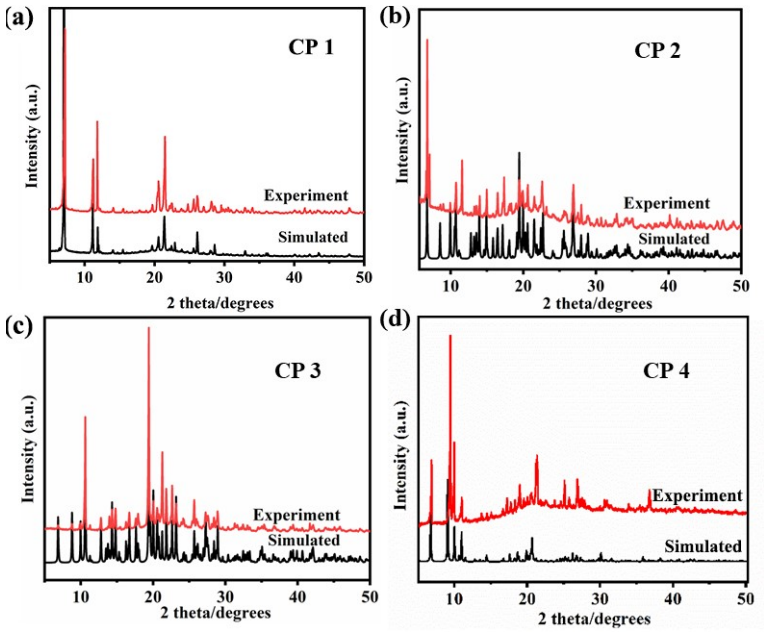

Figure S2. The experimental and simulated X-ray powder diffraction of CPs **1**–**4**.

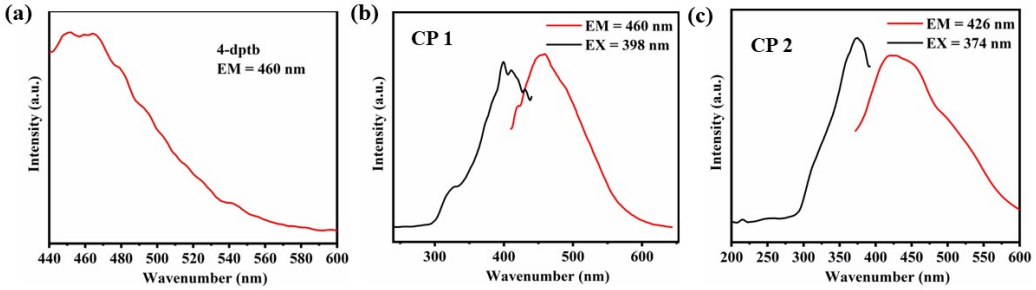

Figure S3. Solid-state fluorescence spectra of CPs **1**–**2** and 4-dptb.

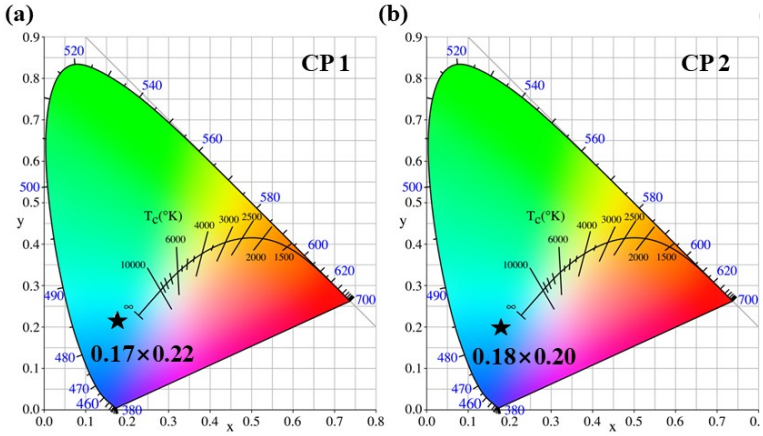

Figure S4. CIE chromaticity diagrams of CPs **1**–**2**.

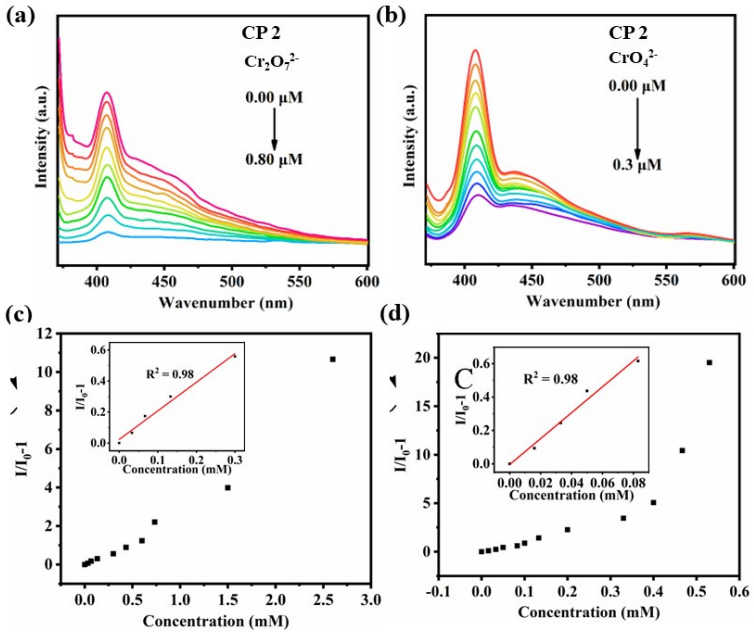

Figure S5. The fluorescence spectra of CP 2 with different concentrations of **(a)** $Cr_2O_7^{2-}$ and **(b)** CrO_4^{2-} anions; the Ksv plot of CP **2** for sensing of **(c)** $Cr_2O_7^{2-}$ and **(d)** CrO_4^{2-} anions (insert: S−V plots at low concentrations).

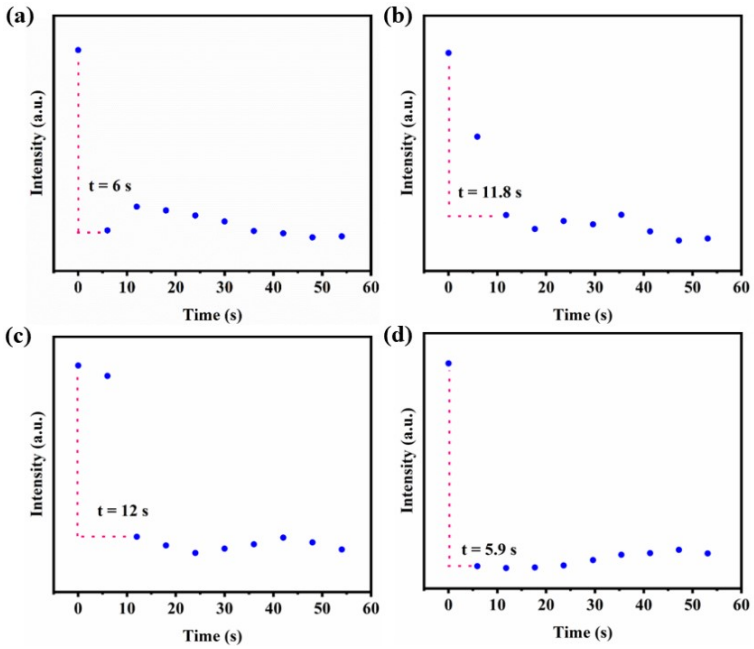

Figure S6. Time-dependent luminescence curve of CPs **1**–**2** after addition of **(a-b)** $Cr_2O_7^{2-}$ and **(c-d)** CrO_4^{2-} anions.

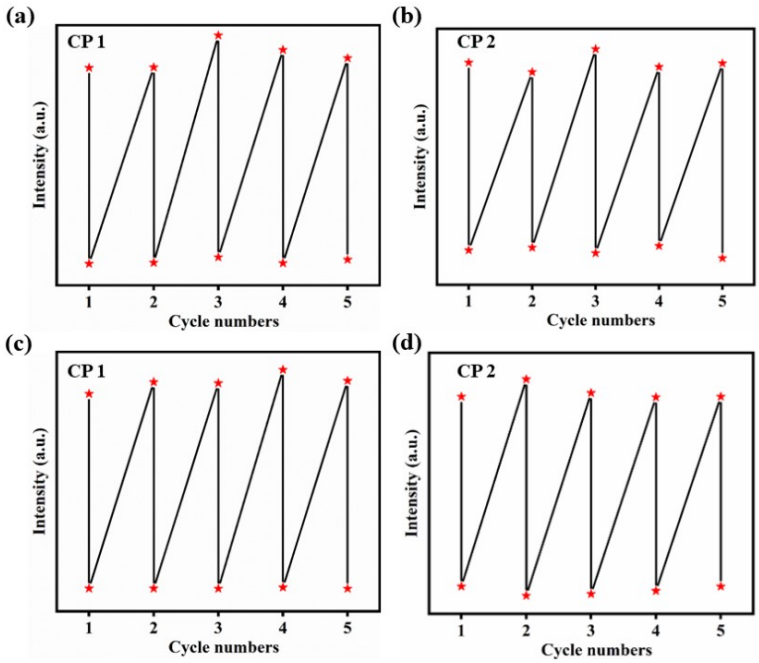

Figure S7. Recyclability for sensing **(a-b)** $Cr_2O_7^{2-}$ and **(c-d)** CrO_4^{2-} anions of CPs **1**–**2** with five continuously quenching cycles.

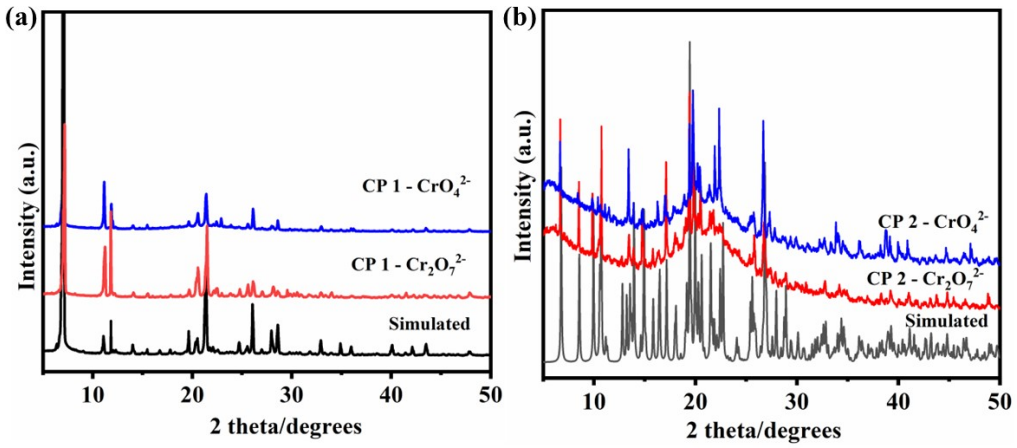

Figure S8. The PXRD patterns of CPs **1**–**2** before and after exposure to different analyzes.

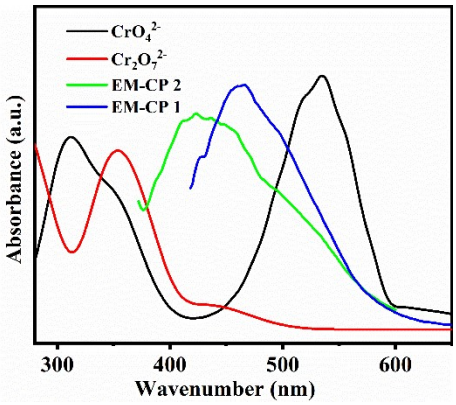

Figure S9. UV-vis absorption spectra of analytes along with the emission spectra of CPs **1**–**2**.

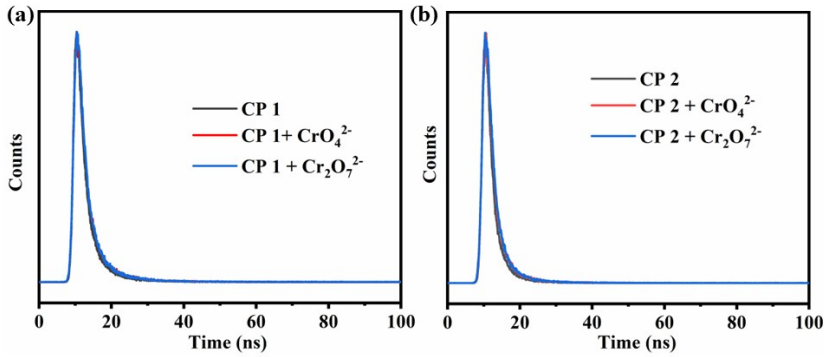

Figure S10. Lifetime decay curves of CPs **1**–**2** before and after the addition of analytes.

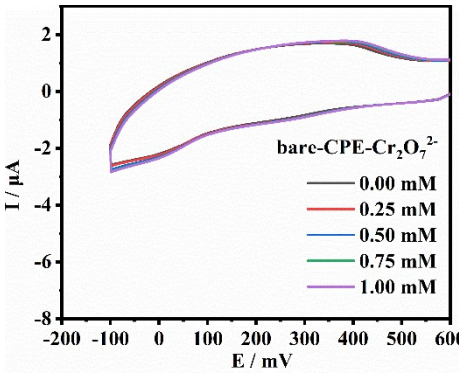

Figure S11. The cyclic voltammogram of bare-CPE in a buffer solution containing different concentrations of $Cr_2O_7^{2-}$ ions (Scan rate: 60 mV s^{-1}).

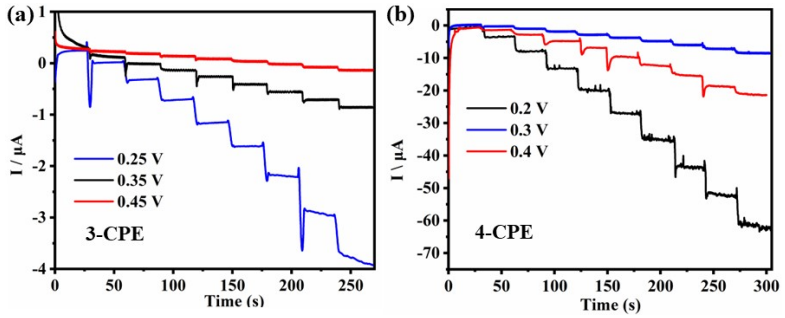

Figure S12. Amperometric current responses of CPs **3**–**4**-CPE upon addition of $Cr_2O_7^{2-}$ ions.

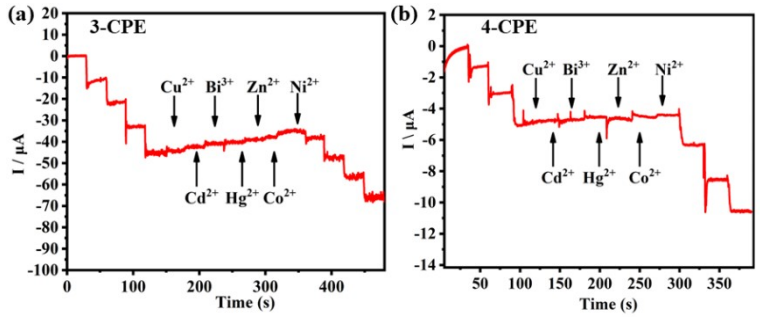

Figure S13. Amperometric current responses of CPs **3**–**4**-CPE in a buffer solution containing $Cr_2O_7^{2-}$ ions with successive additions of 100 µM of various metal ions.